Kayvan R. Keshari,[1,2] David M. Wilson,[3] Victor Sai,[3] Robert Bok,[3] Kuang-Yu Jen,[3] Peder Larson,[3] Mark Van Criekinge,[3] John Kurhanewicz,[3] and Zhen J. Wang[3]

Noninvasive In Vivo Imaging of Diabetes-Induced Renal Oxidative Stress and Response to Therapy Using Hyperpolarized ^{13}C Dehydroascorbate Magnetic Resonance

Oxidative stress has been proposed to be a unifying cause for diabetic nephropathy and a target for novel therapies. Here we apply a new endogenous reduction-oxidation (redox) sensor, hyperpolarized (HP) ^{13}C dehydroascorbate (DHA), in conjunction with MRI to noninvasively interrogate the renal redox capacity in a mouse diabetes model. The diabetic mice demonstrate an early decrease in renal redox capacity, as shown by the lower in vivo HP ^{13}C DHA reduction to the antioxidant vitamin C (VitC), prior to histological evidence of nephropathy. This correlates with lower tissue reduced glutathione (GSH) concentration and higher NADPH oxidase 4 (Nox4) expression, consistent with increased superoxide generation and oxidative stress. ACE inhibition restores the HP ^{13}C DHA reduction to VitC with concomitant normalization of GSH concentration and Nox4 expression in diabetic mice. HP ^{13}C DHA enables rapid in vivo assessment of altered redox capacity in diabetic renal injury and after successful treatment.

Diabetes (type 1 and type 2) currently affects 8.3% of the population in the U.S. (1). Diabetic nephropathy develops in about one-third of diabetic patients and is one of the most devastating complications from diabetes (2). In diabetes, chronic hyperglycemia leads to excessive production of reactive oxygen species (ROS), exceeding local antioxidant capacity and leading to oxidative stress. Oxidative stress has been proposed to be a unifying cause for the onset and progression of diabetic nephropathy, and a target for novel therapies (3–7).

The link among diabetes, oxidative stress, and renal injury has been illustrated in many studies. A primary source of ROS and oxidative stress in renal cells is NAPDH oxidase 4 (Nox4; EC 1.6.3.1), which is activated by chronic hyperglycemia (8–13). Nox4 belongs to a family of enzymes responsible for the production of ROS (superoxide) by transferring electrons across the membrane from NADPH to molecular oxygen. Other isoforms of the Nox family expressed in the kidneys include Nox1 and Nox2, but these are much less abundant in comparison with Nox4. Nox4-dependent superoxide generation and oxidative stress have been shown to mediate glomerular hypertrophy and mesangial matrix accumulation (8,14), which are key histological features of diabetic nephropathy. Nox4-induced oxidative stress also contributes to tubulointerstitial fibrosis seen in diabetic nephropathy (15,16). ACE inhibitors and angiotensin receptor blockers, commonly used classes of drugs used to treat diabetic kidney disease, are thought to protect the kidneys in part by suppressing Nox4-mediated superoxide generation (17,18).

[1]Department of Radiology, Memorial Sloan Kettering Cancer Center, New York, NY

[2]Molecular Pharmacology and Chemistry Program, Memorial Sloan Kettering Cancer Center, New York, NY

[3]Department of Radiology & Biomedical Imaging, University of California, San Francisco, San Francisco, CA

Corresponding author: Kayvan R. Keshari, rahimikk@mskcc.org.

Given the major role of oxidative stress in diabetes, a noninvasive strategy to interrogate oxidative stress in vivo may further enhance our understanding of diabetic renal injury. Such a strategy may also improve the monitoring of the onset and progression of diabetic nephropathy and, importantly, provide biomarkers for response to new therapies.

Hyperpolarized (HP) ^{13}C magnetic resonance (MR) spectroscopy is a new molecular imaging technique that allows noninvasive investigation of dynamic metabolic and physiological processes in real time (19). Hyperpolarization, achieved through the dynamic nuclear polarization technique (20), can provide dramatic enhancement of the ^{13}C nuclear MR signals (>50,000-fold at 3 T) of the substrates as well as subsequent metabolic products. Recently, we developed HP ^{13}C dehydroascorbate (DHA) as an endogenous reduction-oxidation (redox) sensor (21). DHA is an oxidized form of vitamin C (VitC); it is rapidly taken up by cells via the GLUT1, GLUT3, and GLUT4 transporters (22) and is reduced to VitC via a glutathione-dependent mechanism, with coupled reactions with NADPH (Fig. 1). Glutathione, which usually exists in its reduced form (GSH), functions as a key antioxidant by scavenging ROS. It follows that the rate of DHA reduction to VitC reflects cellular redox capacity (23), and serves as an indicator for oxidative stress. We have previously observed rapid in vivo conversion of HP ^{13}C DHA to ^{13}C VitC in tissues expected to be rich in GSH, such as in the kidneys, liver, and brain, and in prostate cancer in a TRAMP (transgenic adenocarcinoma of the mouse prostate) model (21,24).

In this study, we apply HP ^{13}C DHA to interrogate the renal redox capacity in a mouse model of type 2 diabetes and diabetic nephropathy. We show lower HP ^{13}C DHA reduction to ^{13}C VitC during the development of diabetic kidney injury, and its normalization after treatment with an ACE inhibitor (ramipril). HP ^{13}C DHA reduction to VitC reflects the intracellular GSH concentrations and provides a noninvasive probe for monitoring redox alterations in vivo.

RESEARCH DESIGN AND METHODS

Animals

All procedures were approved by the Institutional Animal Care and Use Committee. Male mice homozygous for the leptin receptor mutation (BKS.Cg-*lepr*^{db}/*lepr*^{db} [*db/db* mice]) and their age-matched control littermates (BKS.Cg-*lepr*^{db}/+ [*db/m* mice]) were purchased from The Jackson Laboratory (Bar Harbor, ME). The *db/db* mice are one of the most commonly used murine models of human type 2 diabetes and diabetic nephropathy. The animals were allowed free access to standard chow and drinking water ad libitum. The *db/db* mice at 8, 12, and 16 weeks of age (*n* = 5 for each age group), and their age-matched *db/m* mice (*n* = 4 for each age group) underwent MRI studies, and subsequent histological and biochemical assays described below. In addition, a separate group of *db/db* mice (*n* = 5) were treated with an ACE inhibitor, ramipril (Sigma-Aldrich; 10 mg/kg daily via drinking water) from 8 to 12 weeks of age, followed by MRI and tissue analysis. Contemporaneous 24-h urine samples were collected from the mice for determination of urine albumin excretion by ELISA (Albuwell; Exocell, Philadelphia, PA). Urine 8-hydroxy-2′-deoxyguanosine (8-OHdG) concentrations were measured using a competitive ELISA kit (OxiSelect Oxidative DNA Damage ELISA Kit; Cell Biolabs, San Diego, CA) as previously described (14). Urinary 8-OHdG excretion was expressed as a total amount in nanograms over 24 h. Fasting blood glucose levels of the mice were also measured at the time of the MRI (AlphaTRAK; Abbott Laboratories).

HP ^{13}C MRI Studies

The *db/db* mice and their control littermates *db/m* mice were fasted for 6 h prior to image acquisition. A tail vein catheter was placed for intravascular access. A 2.2 mol/L solution of [1-^{13}C]DHA in dimethyacetamide containing 15 mmol/L OX063 trityl radical (Oxford Instruments) was HP on a HyperSense dynamic nuclear polarization instrument (Oxford Instruments). The frozen sample was
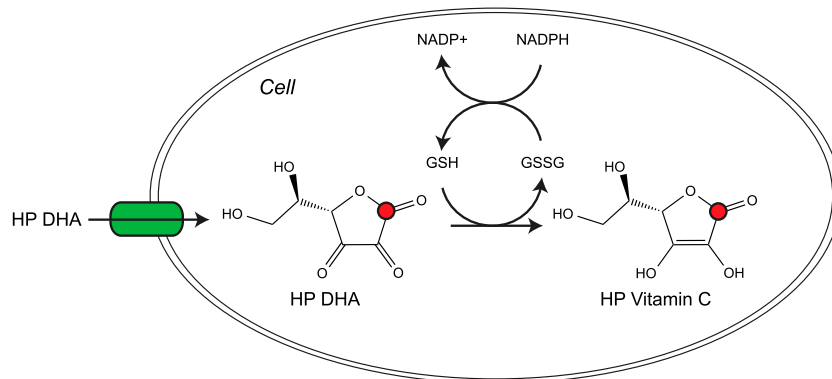
Figure 1—Schematic representation of HP DHA uptake and its subsequent reduction to VitC. The green box indicates GLUT1. DHA is reduced to VitC by DHA reductase (EC 1.8.5.1) in a glutathione-dependent mechanism via coupled reaction to NADPH.

dissolved in distilled water containing 0.3 mmol/L EDTA. Imaging was performed using a 3-T MRI scanner (GE Healthcare, Waukesha, WI) equipped with a multinuclear spectroscopy hardware package. The radiofrequency coil used in these experiments was a dual-tuned ^{1}H-^{13}C coil with a quadrature ^{13}C and ^{1}H channels. Prior to ^{13}C studies, three-plane T$_2$-weighted images were acquired for anatomic localization (echo time 100 ms; repetition time 4 s; six averages) using a standard fast spin echo sequence. ^{13}C MR spectroscopic imaging studies were then acquired 25 s postinjection of 15 mmol/L HP ^{13}C DHA, at 5-mm isotropic resolution, as previously published (21,24).

Histological Evaluation
Two-micrometer-thick renal sections were cut from 10% formalin-fixed, paraffin-embedded kidney samples, and stained with periodic acid Schiff (PAS). Each section was scanned at high magnification ($\times$400) to produce digitized whole slide images and was loaded into the ImageJ software (National Institutes of Health). Ten randomly selected glomeruli in the outer cortex were selected. The percent glomerular mesangial area was calculated as the fraction of the total glomerular tuft cross-sectional area, as previously described (25). 8-OHdG immunostaining of the renal slices was performed using anti–8-OHdG mouse monoclonal antibody (Santa Cruz Biotechnology). In brief, ethanol-fixed sections were prepared, and antigen retrieval was performed using a microwave. Antibodies against 8-OHdG were used for the primary reactions followed by secondary reactions with biotin-labeled anti-mouse goat IgG.

Glutathione Measurements
Renal tissues were homogenized in PBS with EDTA. Protein was precipitated with 10% metaphosphoric acid, and glutathione concentrations were assayed spectrophotometrically using a commercially available 5,5′-dithio-bis-2-(nitrobenzoic acid)–based absorbance assay (Cayman Chemical).

Real-Time PCR
Total RNA was isolated from renal tissues from *db/db* (*n* = 4) and *db/m* (*n* = 4) mice using the Qiagen RNeasy Kit, and was reverse transcribed using SuperScript III Reverse Transcriptase (Invitrogen) according to the manufacturer's instructions. Mouse Nox1, Nox2, and Nox4

Invitrogen primers were obtained from Life Technologies, and real-time PCR determination of cDNA amounts was performed. Relative expression to control gene hypoxanthine phosphoribosyltranserase (HPRT) was determined using the ΔCt method.

Statistical Analysis
Student *t* tests and one-way ANOVA with Tukey-Kramer post hoc tests were used to assess the difference between relevant groups using the statistical software package STATA version 8.0. All values are reported as the mean ± SE. A *P* value of <0.05 was considered statistically significant.

RESULTS

db/db Mice Have Lower HP ^{13}C DHA Reduction to VitC
We performed HP ^{13}C DHA MR spectroscopic imaging in *db/db* mice and age-matched *db/m* mice at 8, 12, and 16 weeks. The *db/db* mice have been reported to reliably develop frank hyperglycemia by 8 weeks of age (26). Table 1 summarizes the weight, blood glucose level, and urine albumin excretion in the *db/db* and *db/m* mice in this study. Figure 2*A* shows representative MR spectra for voxels corresponding to kidneys in a *db/m* and a *db/db* mouse at 12 weeks of age after the injection of HP ^{13}C DHA, demonstrating a lower reduction of DHA to VitC in the *db/db* mouse. Figure 2*B* shows VitC/(VitC + DHA) ratios in the kidneys of *db/m* and *db/db* mice at 8, 12, and 16 weeks of age. For *db/m* mice, the VitC/(VitC + DHA) ratios did not change significantly over time. For *db/db* mice, the VitC/(VitC + DHA) ratios were 13%, 35%, and 33% lower compared with the age-matched *db/m* mice at 8, 12, and 16 weeks, respectively (P = 0.02, 0.03, and 0.02, respectively). A significant difference in the VitC/(VitC + DHA) ratios was found among the *db/db* mice of different ages (P = 0.01). Tukey-Kramer post hoc analysis showed the VitC/(VitC + DHA) ratios were significantly lower in the 12- and 16-week-old *db/db* mice compared with those in the 8-week-old *db/db* mice (P < 0.05 for both), but were not significantly different between the 12- and 16-week-old *db/db* mice. PAS stains of the renal slices demonstrated that the percent mesangial matrix area increased over time in the *db/db* mice, at 13.9% for the 8-week-old *db/db* mice, 17.7% for the 12-week-old *db/db* mice, and 20.4% for the 16-week-old *db/db* mice (P = 0.02, one-way ANOVA). The percent mesangial matrix area

Table 1—Body weights and blood glucose and 24-h urine albumin levels in *db/db* and *db/m* mice at various ages

	Age (weeks)	Body weight (g)	Blood glucose (mg/dL)	Urine albumin (μg/24 h)
db/m mice	8	26.7 ± 1.4	146.5 ± 10.2	13.5 ± 5.2
	12	27.0 ± 2.4	135.7 ± 16.5	15.3 ± 3.1
	16	29.9 ± 0.8	145.3 ± 30.1	17.9 ± 5.4
db/db mice	8	35.9 ± 1.6[a]	214.4 ± 17.9[a]	185.4 ± 35.1[a]
	12	46.3 ± 1.4[a]	378.2 ± 25.0[a]	248.2 ± 50.2[a]
	12 (ramipril)	43.4 ± 3.7[a]	370.4 ± 36.2[a]	67.3 ± 20.9[a,b]
	16	48.3 ± 4.7[a]	463.7 ± 102.4[a]	320.1 ± 65.5[a]

Data are mean ± SE; *n* = 4 in each group. [a]*P* < 0.05 vs. age-matched *db/m* mice. [b]*P* < 0.05 vs. age-matched untreated *db/db* mice.
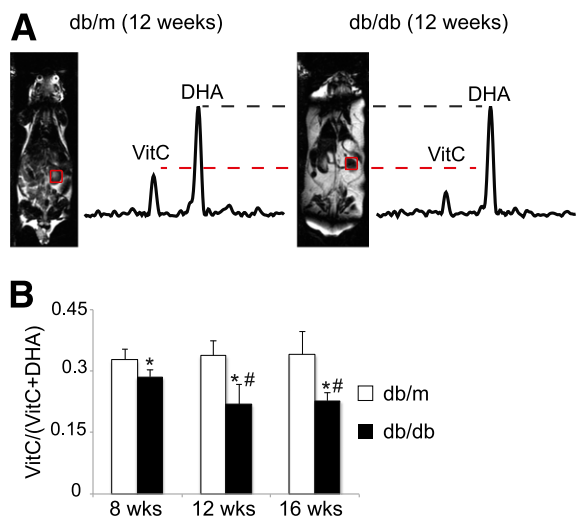
Figure 2—Comparison of HP ^{13}C DHA reduction in *db/m* and *db/db* mice. *A*: Representative HP ^{13}C MR spectra in a 12-week *db/m* and *db/db* mouse. Kidney voxels demonstrate an approximately 50% decrease in VitC production in *db/db* compared with *db/m* mouse. *B*: Renal VitC/(VitC + DHA) ratios in *db/db* and *db/m* mice at 8, 12, and 16 weeks of age. *Significant difference when compared with age-matched *db/m* mice. #Significant difference when compared with 8-week-old *db/db* mice.

was significantly higher in 12- and 16-week-old *db/db* mice compared with 8-week-old *db/db* mice ($P < 0.05$ for both).

db/db Mice Have Decreased Renal GSH and Increased Nox4 Expression Correlating to HP ^{13}C DHA Finding

Since there is a redox coupling mechanism between glutathione and VitC, we hypothesized that the observed in vivo reduction of HP ^{13}C DHA reflects changes in the concentration of GSH. To test this hypothesis, we assayed the kidneys of *db/db* and *db/m* mice for both GSH and oxidized glutathione dimer (GSSG) concentrations using an enzymatic recycling method (27). The results are summarized in Fig. 3. For *db/m* mice, the GSH concentrations did not change significantly among the three time points. For *db/db* mice, the mean renal GSH concentrations were 18%, 26%, and 29% lower compared with age-matched *db/m* mice at 8, 12, and 16 weeks of age, respectively ($P = 0.04$, 0.003, and 0.02, respectively). The renal GSH/GSSG ratios were 27%, 42%, and 38% lower in the *db/db* mice compared with the *db/m* mice at 8, 12, and 16 weeks, respectively ($P = 0.04$, 0.002, and 0.02, respectively). The total glutathione (GSH + GSSG) concentrations in the *db/db* mice were slightly lower than those in the age-matched *db/m* mice, although they did not reach statistical significance ($P = 0.12$, 0.06, and 0.08, respectively). We additionally assayed the mRNA expression of Nox4, which has been shown to be a major source of renal superoxide generation in diabetes (8–13), as well as the expression of Nox1 and Nox2. The renal Nox4 expression was significantly increased in the *db/db* mice compared with *db/m* mice at all three time
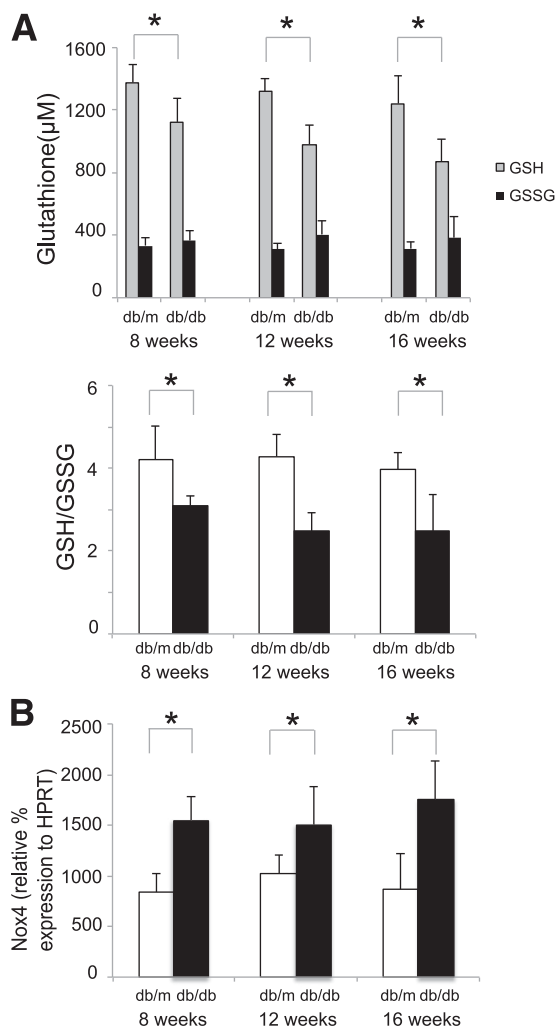
Figure 3—Glutathione and Nox4 in *db/db* and *db/m* mice. *A*: GSH and GSSG concentrations and GSH/GSSG ratios in the kidneys of the *db/m* and *db/db* mice at 8, 12, and 16 weeks of age. The GSH concentrations and GSH/GSSG ratios were significantly lower in *db/db* mice compared with *db/m* mice at all three time points. *B*: Renal Nox4 expression in *db/m* and *db/db* mice at 8, 12, and 16 weeks of age, demonstrating significantly higher Nox4 expression in the *db/db* mice compared with the *db/m* mice. *$P < 0.05$.

points ($P = 0.04$, 0.03, and 0.03 for 8, 12, and 16 weeks, respectively) (Fig. 3). The Nox2 expression was much lower than that of Nox4, and was not significantly different between the *db/db* and *db/m* mice (Supplementary Fig. 1). The Nox1 expression was very low (<1% of the control gene HPRT) in the *db/db* and *db/m* mice (results not shown).

Ramipril Treatment Normalizes Renal HP ^{13}C DHA Reduction to VitC With Corresponding Restoration of GSH Concentration and Nox4 mRNA Expression in *db/db* Mice

Hyperglycemia has been shown to increases cellular angiotensin II (Ang II) production (28), which in turn activates Nox4-mediated superoxide production and oxidative stress (18). We treated a group of *db/db* mice with an ACE inhibitor, ramipril, from 8 to 12 weeks of age and

measured the in vivo HP ^{13}C DHA reduction. We observed that HP ^{13}C DHA reduction to VitC in the kidneys of treated 12-week-old *db/db* mice was restored to a level similar to that found in age-matched *db/m* mice (Fig. 4*A* and *B*). One-way ANOVA with post hoc analysis showed that the VitC/(VitC + DHA) ratios were significantly lower in the 12-week-old untreated *db/db* mice compared with the 12-week-old *db/m* mice ($P < 0.05$) and the 12-week-old treated *db/db* mice ($P < 0.05$). The VitC/(VitC + DHA) ratios were not significantly different between the treated *db/db* mice and the age-matched *db/m* mice. Similar analyses also showed that there were no significant differences between the treated *db/db* mice and the age-matched *db/m* mice with regard to the renal GSH and total glutathione concentrations, GSH/GSSG ratios, and Nox4 mRNA expression level (Fig. 4*C* and *D*). Immunohistochemical stains of 8-OHdG in renal slices demonstrate increased staining, indicating increased oxidative DNA damage, in the untreated *db/db* mice, which is diminished with ramipril treatment (Fig. 4*E*). Similarly, 24-h urine 8-OHdG concentrations were increased in the untreated *db/db* mice, and were normalized to the level in the *db/m* mice after ramipril treatment (Fig. 4*F*). PAS stains of renal slices demonstrate an increased mesangial matrix area in the untreated *db/db* mice, which is diminished with treatment (Fig. 4*G*).

DISCUSSION

Diabetic nephropathy is the major cause of end-stage renal disease. Increased oxidative stress has been proposed to be both a key initiator and a downstream effect of a number of pathways involved in the pathogenesis of diabetic nephropathy. In this study, we monitored, in real time, the renal redox alteration associated with diabetes and after treatment using HP ^{13}C DHA MR. We showed that the *db/db* mice have lower renal HP ^{13}C DHA reduction to VitC compared with age-matched control mice. After 4 weeks of treatment with an ACE inhibitor, ramipril, the *db/db* mice show normalization of the HP ^{13}C DHA reduction to VitC.

The observed alteration in the HP ^{13}C DHA reduction to VitC appears to reflect renal GSH concentration. GSH is the most abundant intracellular thiol-based antioxidant. It protects the cells from oxidative stress by preventing the accumulation of ROS. GSSG, the oxidized form of glutathione, is formed as a product of this detoxification. GSH is regenerated by the action of glutathione reductase (EC 1.8.1.7), an NADPH-dependent enzyme, thus completing the redox cycle. GSH is also a cofactor for the enzyme DHA reductase (EC 1.8.5.1), which recycles DHA back to reduced ascorbic acid (VitC), therefore linking the redox couple between glutathione and VitC. GSH alterations have been observed in diabetes and diabetic nephropathy. For example, renal mesangial cells exposed to chronic hyperglycemia have significantly decreased GSH concentrations (29). Diabetic patients with microalbuminuria were noted to have lower GSH levels in red blood cells than diabetic subjects without microalbuminuria (30). In agreement with these previous studies, we found significantly lower concentrations of GSH and lower GSH/GSSG ratios in the kidneys of *db/db* mice compared with those of age-matched control mice at all three time points. The observed changes in renal HP ^{13}C DHA reduction to VitC appeared to reflect the changes in GSH concentration. The mean VitC/(VitC + DHA) ratios in the *db/db* mice were 13%, 35%, and 33% lower, respectively, compared with the age-matched *db/m* mice at 8, 12, and 16 weeks of age. Correspondingly, the measured renal GSH concentrations were 18%, 26%, and 29% lower, respectively, in the *db/db* mice compared with age-matched *db/m* mice at 8, 12, and 16 weeks of age.

We noted an early decrease in the renal VitC/(VitC + DHA) ratios in the 8-week-old *db/db* mice. Phenotypically, the 8-week-old *db/db* mice in our study demonstrated increased albuminuria, but no significant glomerular histological changes compared with control mice. As the duration of diabetes increased, the glomerular histological changes, as assessed by mesangial matrix area, became evident, although they remained relatively mild even in the 16-week-old *db/db* mice. Taken together, these findings support the notion that alterations in oxidative stress/redox capacity are an early event and may play a primary role in the development of diabetic nephropathy (6,15,31). Noninvasive techniques such as HP ^{13}C DHA MR may facilitate future work to better understand diabetic renal injury, such as the role that oxidative stress plays in determining susceptibility to diabetic nephropathy, as suggested by a previous study (32), and the temporal relationship between oxidative stress and the development of kidney injury.

Nox4 is an enzyme that has been reported to be a major source of renal ROS in diabetes. Upregulation of Nox4 together with increased superoxide generation has been shown in response to high glucose concentration in renal cells and in experimental models of diabetes (8–13). In our study, the observed lower HP ^{13}C DHA reduction to VitC in the kidney of the *db/db* mice corresponded to an increase in Nox4 expression. We postulate that this may be due to Nox4-induced increase in superoxide generation with consumption of GSH (Fig. 5). It should be noted that other sources or pathways are also involved in the increased renal oxidative stress in diabetes. For example, hyperglycemia leads to increased superoxide production by the mitochondrial electron transport chain. This process can in turn activate other superoxide production pathways, such as via Nox4, that may amplify the original damaging effect of hyperglycemia (33). Therefore, other sources of oxidative stress may also contribute to the observed alterations in renal GSH in the diabetic mice. These additional sources likely contribute to the metabolic phenotype reflected in lower HP ^{13}C DHA reduction to VitC in the diabetic kidneys.

It is well recognized that hyperglycemia increases cellular Ang II production (28), which in turn activates
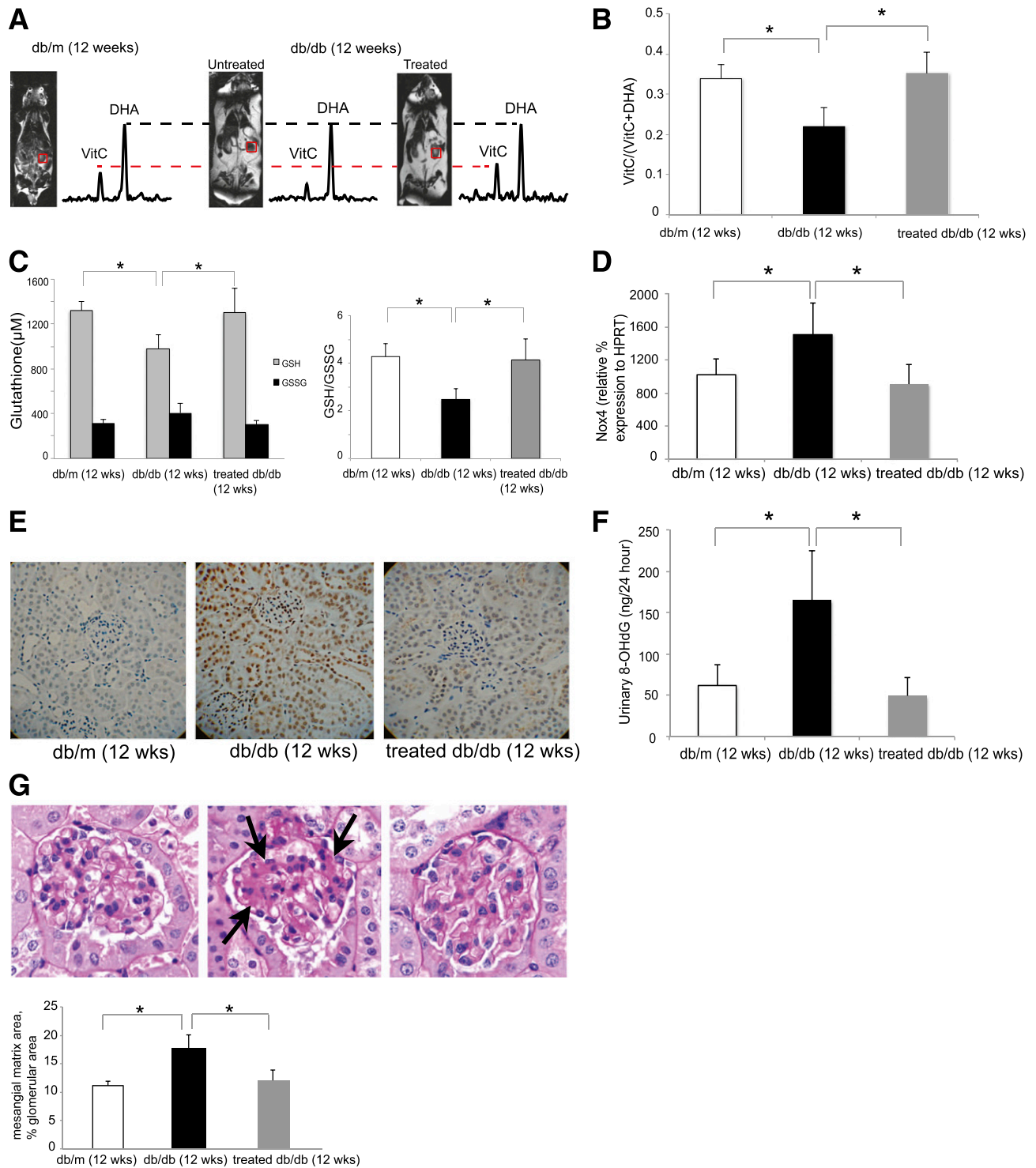
Figure 4—HP ^{13}C DHA reduction and correlative tissue studies in *db/db* mice after ramipril treatment. *A*: Representative HP ^{13}C MR spectra of a 12-week-old *db/m* mouse, an untreated *db/db* mouse, and a *db/db* mouse after 4 weeks of ramipril treatment. Kidney voxels demonstrate normalization of VitC production in the *db/db* mouse after treatment to a level similar to that seen in the *db/m* mouse. Renal VitC/(VitC + DHA) ratios (*B*); renal GSH, GSSG concentrations, and GSH/GSSG ratios (*C*); and renal Nox4 expressions (*D*) demonstrate similar findings. *E*: Representative immunostains of 8-OHdG in renal slices from 12-week-old *db/m* mice, untreated *db/db* mice, and treated *db/db* mice demonstrate increased staining, indicating increased oxidative DNA damage, in the untreated *db/db* mice, which is diminished with ramipril treatment. *F*: Twenty-four–hour urine 8-OHdG concentrations are significantly higher in the untreated *db/db* mice. Ramipril-treated *db/db* mice show urine 8-OHdG concentrations similar to those in the *db/m* mice. *G*: Representative PAS stains of renal slices from 12-week-old *db/m* mice (top left), untreated *db/db* mice (top middle), and treated *db/db* mice (top right), and the percent mesangial matrix area demonstrate increased mesangial matrix area in the untreated *db/db* mice (arrows), which is diminished with ramipril treatment. *P < 0.05.
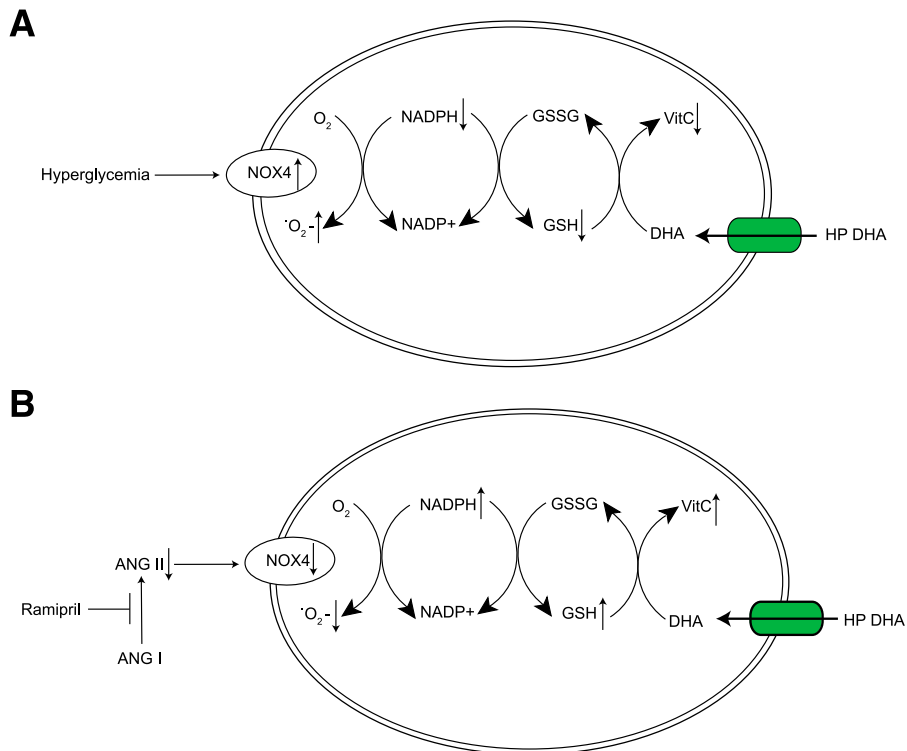
Figure 5—Schematics illustrating the relationships among HP DHA, associated redox pairs, and Nox4. *A*: In response to persistent hyperglycemia, renal Nox4 is upregulated and generates ROS (superoxide) by using NADPH as an electron donor. There is decreased regeneration of GSH from GSSG and decreased reduction of HP DHA to VitC. *B*: Ramipril decreases Ang II production, which in turn decreases Nox4 expression and ROS generation. Via the redox pairs of VitC and GSH, the treatment effect is observed as the normalization of HP DHA reduction to VitC. The green box indicates GLUT1.

Nox4-mediated superoxide production and oxidative stress (18,34). ACE inhibitors, which decrease the production of Ang II, and Ang II receptor blockers are commonly used drugs for the treatment of diabetic nephropathy. They are thought to protect the kidneys in part through the reduction of oxidative stress (35,36) (Fig. 5). In this study, we demonstrated that HP ^{13}C DHA can monitor the targeted effect of an ACE inhibitor (ramipril) on oxidative stress in vivo by observing the HP ^{13}C DHA reduction to VitC. After 4 weeks of ramipril treatment, HP ^{13}C DHA reduction to VitC in the kidneys of 12-week-old *db/db* mice was restored to a level similar to that found in age-matched *db/m* mice. The MR findings parallel the normalization of renal GSH concentration and Nox4 expression. Because of the important role of oxidative stress in the development and progression of diabetic nephropathy as well as other forms of chronic kidney disease (37), new pharmacological strategies that directly or indirectly target oxidative stress are being explored (7,14,38). Noninvasive techniques such as HP ^{13}C DHA MR may provide companion biomarkers that can provide better information on drug targeting and enhance treatment monitoring.

It should be pointed out that, in general, cellular DHA uptake may be facilitated by several factors such as insulin, cyclic adenosine monophosphate, and colony-stimulating factors (39–41) and suppressed by homocysteine (42). Such factors may potentially influence DHA uptake into the renal cells of *db/db* mice with hyperinsulinemia and insulin resistance. Additionally, different cell types within the renal glomeruli and tubules may differentially reduce DHA to VitC due to different insulin sensitivity or resistance. Therefore, future in vitro cell studies using HP ^{13}C DHA are warranted to elucidate the uptake and reduction of DHA in different renal cells in a diabetic milieu. It should also be noted that DHA reduction to VitC can be affected by enzymes such as glutaredoxin (Glrx) and glutathione *S*-transferase ω (GSTO) that have DHA reductase activity (43,44). The mRNA expressions of Glrx-1 and GSTO-1, were noted to be higher in the *db/db* mice compared with the *db/m* mice (Supplementary Fig. 2). Therefore, the observed lower renal HP ^{13}C DHA reduction to VitC in the *db/db* mice compared with the *db/m* mice cannot be explained by the alterations of expression of these enzymes. Future studies are needed to investigate the role that other enzymes play in the HP ^{13}C DHA reduction to VitC.

There are presently limited noninvasive in vivo methods for measuring oxidative stress in the kidneys. Urine markers of oxidative stress, such as 8-OHdG (a marker of DNA oxidative damage), have been used to study

diabetes-associated oxidative stress (45). Ex vivo measurement of such markers, however, can be adversely affected by variables, such as how the samples are collected and stored (46), and may not accurately reflect oxidative stress in real time at the tissue level. Electron spin resonance (ESR) imaging has been applied to detect free radicals in the kidneys in vivo (47). However, the sensitivity of the ESR instruments for in vivo studies and the specificity and stability of the probes are presently insufficient (48). A recent study reported in vivo imaging of immunospin-trapped radicals with MRI in a mouse diabetes model (49). A drawback of this technique is that it required multiple injections to trap radicals over the course of days (49). Both the ESR imaging and immunospin-trapped radical MRI assess oxidative stress by measuring radical levels.

HP ^{13}C DHA MR provides a different approach of determination of oxidative stress via real-time evaluation of the redox capacity in vivo. In this preclinical study, because of the small size of the mouse kidneys, the spatial resolution of the HP ^{13}C DHA MR does not currently allow for separate evaluation of the renal cortex and medulla. Several approaches will address this problem, including better substrate polarization and coil design, and more efficient sampling of k-space. These advances will allow specific interrogation of the various renal compartments in preclinical models, as well as in potential future clinical studies. An important consideration in the clinical translation of HP ^{13}C probes is that injection of probes at doses in the micromolar-to-millimolar range is necessary to achieve sufficient MR signals. While probes such as ^{13}C DHA have the advantage of being an endogenous compound, the metabolic effects of the injected dose and the safety in humans will need to be established. Notably, the clinical translation of HP ^{13}C MR technology has been recently achieved with the successful completion of the phase I clinical trial of HP ^{13}C pyruvate in prostate cancer patients (50), which opens doors for potential clinical translation of other endogenous HP probes such as DHA.

In conclusion, our study has shown that HP ^{13}C DHA reduction to VitC correlates to the GSH component of the redox couple, and likely reflects the impact of diabetes-induced alterations in renal superoxide generation and oxidative stress. HP ^{13}C DHA can, in real time, noninvasively probe the redox changes associated with diabetic renal injury and after successful treatment. Such an imaging approach may potentially enhance the prediction and early detection of diabetic nephropathy and provide companion biomarkers that can better inform on the response to new therapies targeting oxidative stress in patients. More broadly, such imaging strategies can be extended to the noninvasive in vivo evaluation of other complications from diabetes as well as other oxidative stress-related diseases.

References

1. American Diabetes Association. Statistics about diabetes: data from the National Diabetes Statistics Report, 2014 (released June 10, 2014) [article online], 2014. Available from http://www.diabetes.org/diabetes-basics/diabetes-statistics/. Accessed 10 June 2014

2. Caramori ML, Mauer M. Diabetes and nephropathy. Curr Opin Nephrol Hypertens 2003;12:273–282

3. Rösen P, Nawroth PP, King G, Möller W, Tritschler HJ, Packer L. The role of oxidative stress in the onset and progression of diabetes and its complications: a summary of a Congress Series sponsored by UNESCO-MCBN, the American Diabetes Association and the German Diabetes Society. Diabetes Metab Res Rev 2001;17:189–212

4. Nishikawa T, Edelstein D, Du XL, et al. Normalizing mitochondrial superoxide production blocks three pathways of hyperglycaemic damage. Nature 2000;404:787–790

5. Forbes JM, Coughlan MT, Cooper ME. Oxidative stress as a major culprit in kidney disease in diabetes. Diabetes 2008;57:1446–1454

6. Brownlee M. The pathobiology of diabetic complications: a unifying mechanism. Diabetes 2005;54:1615–1625

7. Zheng H, Whitman SA, Wu W, et al. Therapeutic potential of Nrf2 activators in streptozotocin-induced diabetic nephropathy. Diabetes 2011;60:3055–3066

8. Gorin Y, Block K, Hernandez J, et al. Nox4 NAD(P)H oxidase mediates hypertrophy and fibronectin expression in the diabetic kidney. J Biol Chem 2005;280:39616–39626

9. Block K, Gorin Y, Abboud HE. Subcellular localization of Nox4 and regulation in diabetes. Proc Natl Acad Sci U S A 2009;106:14385–14390

10. Sedeek M, Callera G, Montezano A, et al. Critical role of Nox4-based NADPH oxidase in glucose-induced oxidative stress in the kidney: implications in type 2 diabetic nephropathy. Am J Physiol Renal Physiol 2010;299:F1348–F1358

11. Gorin Y, Block K. Nox4 and diabetic nephropathy: with a friend like this, who needs enemies? Free Radic Biol Med 2013;61C:130–142

12. Gorin Y, Block K. Nox as a target for diabetic complications. Clin Sci (Lond) 2013;125:361–382

13. Thallas-Bonke V, Thorpe SR, Coughlan MT, et al. Inhibition of NADPH oxidase prevents advanced glycation end product-mediated damage in diabetic nephropathy through a protein kinase C-α-dependent pathway. Diabetes 2008;57:460–469

14. Fujii M, Inoguchi T, Maeda Y, et al. Pitavastatin ameliorates albuminuria and renal mesangial expansion by downregulating NOX4 in db/db mice. Kidney Int 2007;72:473–480

15. Singh DK, Winocour P, Farrington K. Oxidative stress in early diabetic nephropathy: fueling the fire. Nat Rev Endocrinol 2011;7:176–184

16. Kanwar YS, Sun L, Xie P, Liu FY, Chen S. A glimpse of various pathogenetic mechanisms of diabetic nephropathy. Annu Rev Pathol 2011;6:395–423

17. Sato-Horiguchi C, Ogawa D, Wada J, et al. Telmisartan attenuates diabetic nephropathy by suppressing oxidative stress in db/db mice. Nephron Exp Nephrol 2012;121:e97–e108

18. Kim SM, Kim YG, Jeong KH, et al. Angiotensin II-induced mitochondrial Nox4 is a major endogenous source of oxidative stress in kidney tubular cells. PLoS One 2012;7:e39739

19. Keshari KR, Wilson DW. The chemistry and biochemistry of 13C hyperpolarized magnetic resonance using dynamic nuclear polarization. Chem Soc Rev 2014;43:1627–1659

20. Ardenkjaer-Larsen JH, Fridlund B, Gram A, et al. Increase in signal-to-noise ratio of > 10,000 times in liquid-state NMR. Proc Natl Acad Sci U S A 2003;100: 10158–10163

21. Keshari KR, Kurhanewicz J, Bok R, Larson PE, Vigneron DB, Wilson DM. Hyperpolarized ^{13}C dehydroascorbate as an endogenous redox sensor for in vivo metabolic imaging. Proc Natl Acad Sci U S A 2011;108:18606–18611

22. Liang WJ, Johnson D, Jarvis SM. Vitamin C transport systems of mammalian cells. Mol Membr Biol 2001;18:87–95

23. Ghiselli A, Serafini M, Natella F, Scaccini C. Total antioxidant capacity as a tool to assess redox status: critical view and experimental data. Free Radic Biol Med 2000;29:1106–1114

24. Keshari KR, Sai V, Wang ZJ, Vanbrocklin HF, Kurhanewicz J, Wilson DM. Hyperpolarized [1-13C]dehydroascorbate MR spectroscopy in a murine model of prostate cancer: comparison with 18F-FDG PET. J Nucl Med 2013;54:922–928

25. Cohen MP, Lautenslager GT, Shearman CW. Increased urinary type IV collagen marks the development of glomerular pathology in diabetic d/db mice. Metabolism 2001;50:1435–1440

26. Sharma K, McCue P, Dunn SR. Diabetic kidney disease in the db/db mouse. Am J Physiol Renal Physiol 2003;284:F1138–F1144

27. Rahman I, Kode A, Biswas SK. Assay for quantitative determination of glutathione and glutathione disulfide levels using enzymatic recycling method. Nat Protoc 2006;1:3159–3165

28. Gabriely I, Yang XM, Cases JA, Ma XH, Rossetti L, Barzilai N. Hyperglycemia modulates angiotensinogen gene expression. Am J Physiol Regul Integr Comp Physiol 2001;281:R795–R802

29. Catherwood MA, Powell LA, Anderson P, McMaster D, Sharpe PC, Trimble ER. Glucose-induced oxidative stress in mesangial cells. Kidney Int 2002;61:599–608

30. Ozdemir G, Ozden M, Maral H, Kuskay S, Cetinalp P, Tarkun I. Malondialdehyde, glutathione, glutathione peroxidase and homocysteine levels in type 2 diabetic patients with and without microalbuminuria. Ann Clin Biochem 2005;42:99–104

31. Koya D, Hayashi K, Kitada M, Kashiwagi A, Kikkawa R, Haneda M. Effects of antioxidants in diabetes-induced oxidative stress in the glomeruli of diabetic rats. J Am Soc Nephrol 2003;14(Suppl. 3):S250–S253

32. Beisswenger PJ, Drummond KS, Nelson RG, Howell SK, Szwergold BS, Mauer M. Susceptibility to diabetic nephropathy is related to dicarbonyl and oxidative stress. Diabetes 2005;54:3274–3281

33. Giacco F, Brownlee M. Oxidative stress and diabetic complications. Circ Res 2010;107:1058–1070

34. Griendling KK, Minieri CA, Ollerenshaw JD, Alexander RW. Angiotensin II stimulates NADH and NADPH oxidase activity in cultured vascular smooth muscle cells. Circ Res 1994;74:1141–1148

35. Forbes JM, Cooper ME, Thallas V, et al. Reduction of the accumulation of advanced glycation end products by ACE inhibition in experimental diabetic nephropathy. Diabetes 2002;51:3274–3282

36. Yoshida S, Hashimoto T, Kihara M, et al. Urinary oxidative stress markers closely reflect the efficacy of candesartan treatment for diabetic nephropathy. Nephron Exp Nephrol 2009;111:e20–e30

37. Shah SV, Baliga R, Rajapurkar M, Fonseca VA. Oxidants in chronic kidney disease. J Am Soc Nephrol 2007;18:16–28

38. Hsu SP, Chiang CK, Yang SY, Chien CT. N-acetylcysteine for the management of anemia and oxidative stress in hemodialysis patients. Nephron Clin Pract 2010;116:c207–c216

39. Siushansian R, Tao L, Dixon SJ, Wilson JX. Cerebral astrocytes transport ascorbic acid and dehydroascorbic acid through distinct mechanisms regulated by cyclic AMP. J Neurochem 1997;68:2378–2385

40. Qutob S, Dixon SJ, Wilson JX. Insulin stimulates vitamin C recycling and ascorbate accumulation in osteoblastic cells. Endocrinology 1998;139:51–56

41. Vera JC, Rivas CI, Zhang RH, Golde DW. Colony-stimulating factors signal for increased transport of vitamin C in human host defense cells. Blood 1998;91: 2536–2546

42. Park JB. Reduction of dehydroascorbic acid by homocysteine. Biochim Biophys Acta 2001;1525:173–179

43. Wells WW, Xu DP, Yang YF, Rocque PA. Mammalian thioltransferase (glutaredoxin) and protein disulfide isomerase have dehydroascorbate reductase activity. J Biol Chem 1990;265:15361–15364

44. Whitbread AK, Masoumi A, Tetlow N, Schmuck E, Coggan M, Board PG. Characterization of the omega class of glutathione transferases. Methods Enzymol 2005;401:78–99

45. Broedbaek K, Siersma V, Henriksen T, et al. Urinary markers of nucleic acid oxidation and long-term mortality of newly diagnosed type 2 diabetic patients. Diabetes Care 2011;34:2594–2596

46. Morrow JD, Roberts LJ 2nd. Quantification of noncyclooxygenase derived prostanoids as a marker of oxidative stress. Free Radic Biol Med 1991;10:195–200

47. Sonta T, Inoguchi T, Matsumoto S, et al. In vivo imaging of oxidative stress in the kidney of diabetic mice and its normalization by angiotensin II type 1 receptor blocker. Biochem Biophys Res Commun 2005;330:415–422

48. Han JY, Hong JT, Oh KW. In vivo electron spin resonance: an effective new tool for reactive oxygen species/reactive nitrogen species measurement. Arch Pharm Res 2010;33:1293–1299

49. Towner RA, Smith N, Saunders D, et al. In vivo imaging of immuno-spin trapped radicals with molecular magnetic resonance imaging in a diabetic mouse model. Diabetes 2012;61:2405–2413

50. Nelson SJ, Kurhanewicz J, Vigneron DB, et al. Metabolic imaging of patients with prostate cancer using hyperpolarized [1-13C]pyruvate. Sci Transl Med 2013; 5:198ra108